International Journal of Nanoelectronics and Materials
IJNeaM
ISSN 1985-5761 | E-ISSN 2232-1535

Influence of Zinc Oxide Nanoparticles on the Efficiency of Oxytetracycline Removal from Wastewater Using Continuous Catalytic Ozonation

Sarmad Al-Anssari[a,b,c,*], Hassanain A. Hassan[a], Maha K. Mohsin[d] and Ahmed A. Mohammed[d]

[a]*Department of Chemical Engineering, College of Engineering, University of Baghdad, Iraq*
[b]*Department of Petroleum Engineering, College of Engineering, Al-Naji University, Iraq*
[c]*School of Engineering, Edith Cowan University, Joondalup, Australia*
[d]*Department of Environmental Engineering, College of Engineering, University of Baghdad, Iraq*
**Corresponding author. E-mail: al-anssari@uobaghdad.edu.iq*

ABSTRACT

Antibiotics must be fully eliminated before they are released into the environment. In most cases, conventional wastewater treatment systems are not built to handle polar microcontaminants such as antibiotics. Oxytetracycline (OTC) is one of these antibiotics, an environmental hazard contaminant in aqueous solutions. Therefore, an advanced treatment method is needed for wastewater contaminated with antibiotics. In this study, we employed zinc oxide nanoparticles (ZnO), and the catalytic ozonation procedure was employed to increase the ozonation efficiency. A continuous experiment was carried out to compare the effectiveness of catalytic and single ozonation in degrading OTC in a continuous reactor. The flow rate of OTC solution, the initial concentration of OTC, the ozone generation rate, and the bed height of the catalyst were investigated. The highest removal was obtained at a low flow rate of OTC solution (3.9 cm^3/s) and with a bed height of 1cm. The first-order model and the rate of the oxidation process were well-matched. The self-decomposition rate constant was found to increase from 0.08 to 0.216 s^{-1} with increasing pH range (e.g., 3 -11 pH). The calculated volumetric mass transfer coefficient of ozone in water increased with pH. Gas Chromatography-mass spectrometry analysis indicated that oleyl alcohol and oleic acid were the byproducts of this process.

Keywords: *Wastewater treatment, Oxytetracycline, Continuous Catalytic Ozonation, ZnO nanoparticles, Removal efficiency*

1. INTRODUCTION

One of the most serious and crucial environmental issues that communities are currently facing is the pollution of water resources by pharmaceutical waste, particularly in areas where communities depend on these sources for drinking water (Mohammed et al., 2020a). The majority of drugs that are released into the environment via pharmacies, the pharmaceutical industry, and human waste are antibiotics (Mohammed et al., 2020c). Pharmaceutical antibiotics' impacts on public health and hazards on water sources are a prominent issue in recent years (Mohammed et al., 2020b, Mohsin and Mohammed, 2021, Hammood and Mohammed, 2024b). Oxytetracycline (OTC), One of the most widely used antibiotics in both human and veterinary medicine, is a member of the tetracycline family, and typically use to treat a variety of infectious disorders, including anthrax, cholera, typhus, malaria, syphilis, and respiratory infections (Zhu et al., 2001, Kim et al., 2005, Sarmah et al., 2006, Li et al., 2008). Although it is commonly used in agricultural practices to improve embryo survival rates, it decomposes naturally very slowly. Such slow decomposition is mainly due to its complex chemical composition. Numerous researchers have therefore sought to develop efficient means of eliminating OTC (Kimera et al., 2015, Kerdnawee et al., 2017) from water sources. Typically, antibiotics were taken out of the water using coagulation, membrane separation, adsorption, and biodegradation methods (Wang et al., 2019a). However, biological treatment methods often take longer than chemical ones and are ineffective for very persistent pollutants (Nashmi et al., 2020, Al-Bayati et al., 2023). Thus, due to their high operational cost and low removal efficiency, they are not widely applied. Therefore, Antibiotics' capacity to inhibit bacteria has been improved by the use of advance oxidation processes (AOPs), which also increased the biodegradability and elimination rate of the antibiotics (Hernandez et al., 2002, Wang et al., 2019a). In this context, AOPs use strong oxidation agents, such as superoxide radical (O_2^-), hydroxyl radical (OH) and ozone (O_3) to remove organic contaminants (Buxton et al., 1988, Wang and Xu, 2012, Wang et al., 2019b, Hammood and Mohammed, 2024a). Different methods were used to produce oxidation agents. AOPs are classified into electrochemical oxidation, ionizing radiation, fenton oxidation, photocatalytic oxidation (Alwared et al., 2023), ozonation, and catalytic ozonation (Wang et al., 2019a). Catalytic ozonation is a promising technique for the removal of various inorganic and organic contamination in water owing to its simplicity and effectiveness (Homem and Santos, 2011, Kerdnawee et al., 2017). Typically, the performance of catalytic ozonation mainly depends on the type, size, and surface properties of the catalyst. Using modifind and an engineered catalyst with unique surface properties, including nano-sized catalysts, can significantly enhance the efficiency of the process.

Nanotechnology, including nanoparticles (NPs) and nanofluids, has drawn attention to its wide potential applications in science, technology, industry, and environmental applications (Al-Anssari, 2018). In this context, the small size, high surface-to-volume ratio, unique design, and surface hydophilicity of NPs have shown potential in a diverse range of projects spanning from medicine, drug delivery, foods, corrosion inhibition, enhanced oil recovery, carbon capture and storage, to environmental applications such as soil decontamination and wastewater treatment (Al-Anssari et al., 2020, Mahdi et al., 2023), on which this study focuses on. The surface properties of NPs can be further adjusted via the addition of active materials to enhance the catalytic properties of such nanomaterials (Balaji et al., 2011).

Nanostructured Zinc oxide (ZnO) materials have gained substantial interest due to their extraordinary performance as catalysts, photo catalysts, antibacterial materials, and in other environmental applications (Roy and Chakraborty, 2021). Since the 1960s, the manufacture of ZnO thin films has been a demanding industry due to its use in various applications, including sensors, transducers, and photocatalysts (Baruah and Dutta, 2009). ZnO nanoparticles (NPs) are gaining a lot of interest due to their antibacterial nature and their bactericidal efficiency increasing with decreased particle size (Padmavathy and Vijayaraghavan, 2008). Such an antibacterial phenomenon of ZnO is mechanistically attributed to the creation of reactive oxygen species on the surface of this oxide. Further, ZnO is utilized as a heterogeneous catalyst because it is non-toxic, has a cheap manufacturing cost, and has a significant potential for usage in water and wastewater treatment (Nasseh et al., 2020). In ozonation treatment, which is based on the creation of radicals (OH), ZnO NPs in the liquid phase can excite ozone to generate hydroxyl radicals (OH) and enhance degradation efficiency (Mohsin and Mohammed, 2021).

This work examined the effects of ZnO NPs in the catalytic ozonation method on the removal of Oxytetracycline from wastewater and compared the results with the case of the sole ozonation process (e.g., without ZnO NPs) in terms of different flow rate of simulated wastewater, initial concentration of OTC, ozone generation rate, catalyst bed highest, the rate constant for ozone self-decomposition and the mass transfer coefficient. This work gives the first insight into the utilization of ZnO NPs on the removal of Oxytetracycline from wastewater.

2. EXPERIMENTAL METHODS

2.1. Materials

Oxytetracycline (OTC) powder ($C_{22}H_{24}N_2O_9$, water solubility > 100 mg/ml, molecular weight 460.4 g/mol, yellow colored) supplied by the general company for the medicines business, Samarra, Iraq. The structure of OTC is depicted in Figure1. To avoid the effect of various lab conditions and potential contamination, the stock and diluted solutions of OTC were made directly at the time of each experiment. In this context, a predetermined amount of OTC powder was dissolved in one liter of distilled water to formulate the OTC remedy. The pH of the aqueous phase was adjusted during the experiments by adding drops of NaOH or HCl accordingly. The zinc oxide NPs (metal oxide spherical NPs with a size range of 30-40 nm, Molecular weight 81.39, surface area 10-25 m^2/g) were purchased from Sigma Aldrich. The X-ray diffraction (XRD) characterization of ZnO NPs, by the supplier, indicated a crystalline and hexagonal structure of the white powder. This was also confirmed via scanning electron microscope (SEM) and transmission electron microscope (TEM) images in previous studies (Mohan and Renjanadevi, 2016). ZnO is classified as a semiconductor and has high thermal and mechanical stability, which makes it a good candidate for catalytic applications.

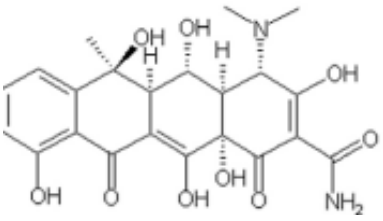

Figure 1. The structure and characteristics of oxy-tetracycline.

2.2. Continuous Experiments: (Ozone +O_2)

The experimental setup included a three-phase reactor where fluidized ZnO NPs catalysts are continually and concurrently flowing upward along with an ozone + oxygen (ozone +O_2) gas mixture. As depicted in Figure 2, a fluidized bed reactor is a cylindrical borosilicate bubble column with an effective height of 1 m and an inner diameter of 5 cm. An ozone generator created ozone from pure oxygen and fed the column with it from the bottom via a diffuser. The studies were conducted at various OTC solution flow rates, beginning OTC concentrations, ozone generation rates, and catalyst bed heights (Mohsin and Mohammed, 2021). The OTC solution and ozone current were applied at the same time in one direction until the liquid achieved steady-state conditions**,** and then, during 35 min, the sample was withdrawn to measure the OTC concentration. The hood gently eliminated the gas phase ozone that was departing the reactor.

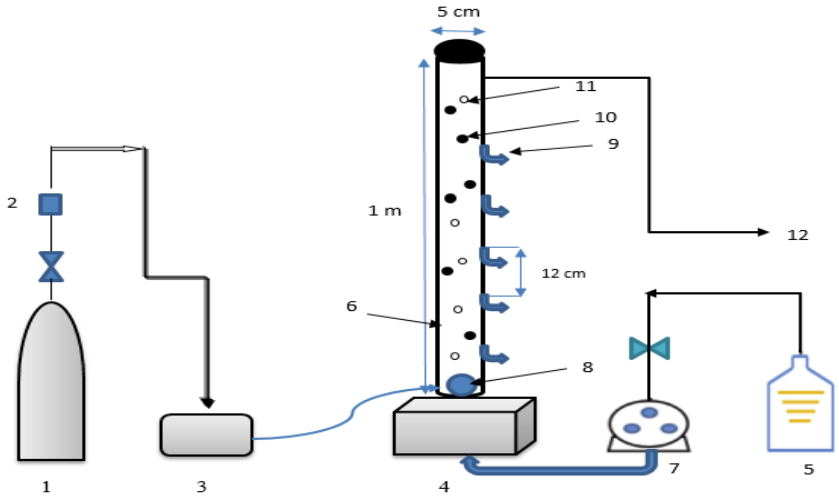

Figure 2. Graphic diagram of the continuous experimental set-up: (1) Oxygen source (2) Flow meter (3) Ozone generator (4) base (5) feed tank for OTC solution (6) bubble column reactor (7) peristaltic pump (8) Diffuser (9) sampling point (10) Catalyst particles (11) ozone bubble (12) outlet solution.

2.3. Changes in Toxicity

Parent compounds of antibiotics would affect the aquatic microbial activity, and after treatment of these antibiotics in different ways, such as ozone and its by-product, they become more toxic. Also, with increasing the concentration of these antibiotics, the toxicity will increase (Li et al., 2008). The poisonous substance's inhibition of bacteria's bioluminescence can be used to explain it. According to Li et al. (2008), the inhibitory efficacy decreases with ozonation time and pH because antibiotics and their by-products of degradation are destroyed.

2.4. Kinetic Study

Understanding the kinetic processes through which organic material, such as drugs and antibiotics, degrades during oxidation treatment procedures is essential. In order to get the best design for the treatment system and effective application of the employed catalyst, the experimental kinetic data must also be accurately modeled using the pertinent theoretical equations. The literature successfully employed the first-order model to the model of degrading data of organic contaminants using a number of treatment strategies (Nasseh et al., 2020). The experimental kinetic data of oxy-tetracycline degradation were simulated using this model. The kinetic investigation made extensive use of the reaction time effect outcomes as feed data. A linear technique is used to calculate the first-order model parameter (Equation 1) and the regression coefficient (R^2). Additionally, Equation 2 is used to determine the half-life time ($t_{1/2}$) of oxytetracycline degradation which corresponds to C_t=50%C_0 .

$$\mathrm{Ln}\left(\frac{C_t}{C_0}\right) = -k_a t \quad (1)$$

$$t_{1/2} = \frac{0.693}{k_a} \quad (2)$$

where k_a (min^{-1}) is the rate constant for a first-order reaction, and t (min) represents the specific reaction time.

3. RESULTS AND DISCUSSION

3.1. Effect of Flow Rate of Solution

Various flow rates (3.9, 8.6, 18.1, 27.5, 36.5, and 42.7 cm^3/s) of solution were pumped at constant concentrations of 50 mg/L, pH=7, and ozone production rate of 1.38 mg/s. At several heights, including 2, 14, 26, 38, 50, and 62 cm, the samples were obtained. As illustrated in Figure 3, it was shown that the removal efficiency increased to 95% at a low flow rate of 3.9 cm^3/s at a height of 62 cm. It's obvious that the longer the liquid residence time, the more reaction time is given for the reaction between ozone and OTC, thus resulting in a higher removal efficiency (Kimera et al., 2015). Subsequently, the removal efficiency decreased when the flow increased. Typically, at high flow, the contact time between the solution and bubble ozone decreases (Al jibouri et al., 2015), thus lower reaction time. Also, it was noted that the removal efficiency only decreased by less than 10% at the higher flow of 42.7cm^3/s. This is a very important observation for treating substantial quantities of contaminated water with OTC.

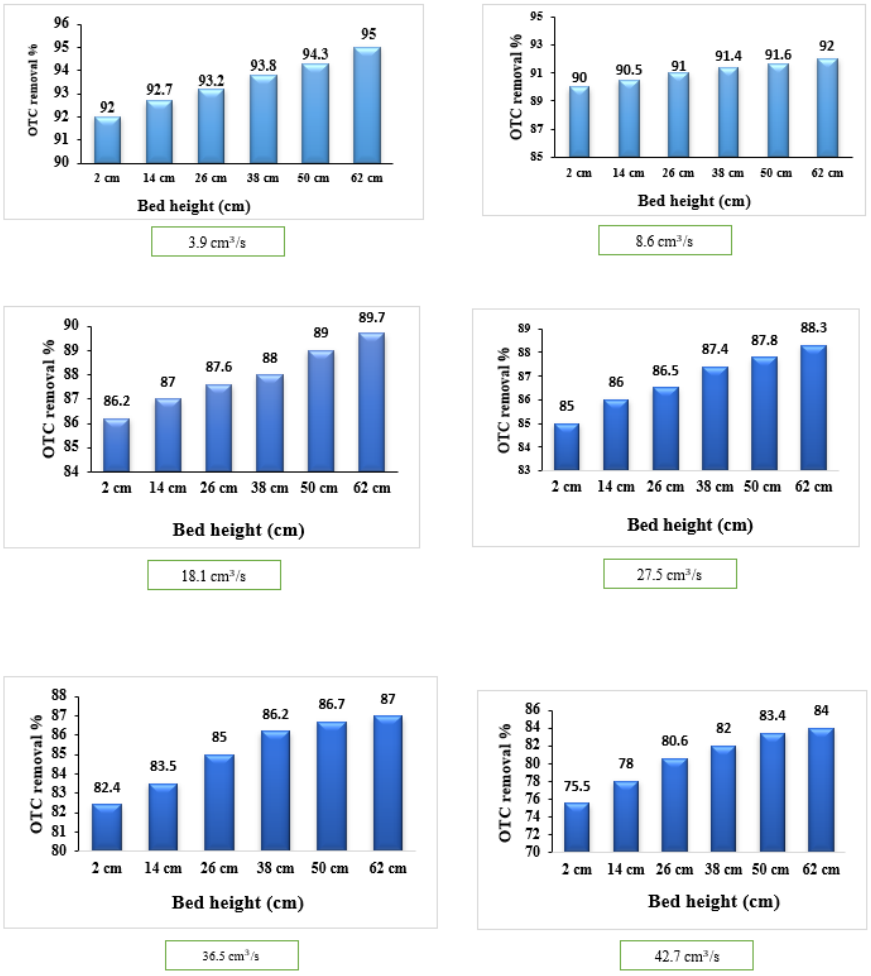

Figure 3. OTC removal efficiency at different solution flow rates.

3.2. Effect of Initial OTC Concentration

Various doses of OTC solution (10, 25, 50, 75, and 100 mg/L) were examined at pH 7, and a constant flow rate of 3.9 cm^3/s. As illustrated in Figure 4, higher initial OTC concentrations result in lower removal efficiency for all tested conditions.

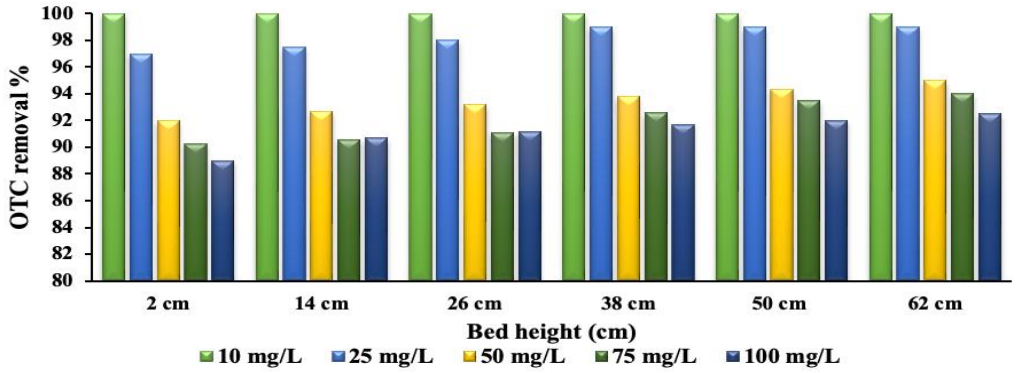

Figure 4. Effect of the initial concentration of OTC on the removal efficiency.

Total removal of OTC was measured at different heights after reaching steady state and with an initial concentration of 10 mg/L. The removal efficiencies were 99%, 95%, 94%, and 92.5% for 25, 50, 75, and 100 mg/L, respectively. Typically, at lower initial concentrations, ozone was able to oxidize more OTC, thus higher removal efficiency was observed. Knowing that the process follows first-order kinetics, therefore, as the concentration of degradation intermediates rises in response to an increase in the initial OTC concentration, more ozone is used for more byproduct oxidation and removal (Sun et al., 2019).

3.3. Effect of Bed Height of Catalyst

The effect of the catalyst (ZnO NPs) bed height (1, 2, and 4 cm) on OTC removal during continuous catalytic ozonation was investigated. With OTC solution concentration of 50 mg/L, pH=7, ozone generation rate =1.38 mg/s, flow rate=3.9cm^3/s and at room temperature. Results are illustrated in Figure 5. Significantly, the removal efficiency reached 98% with only 5g of ZnO (1cm height). Surprisingly, the degradation rate of OTC decreased by increasing the catalyst bed to 2 and 4 cm. In other words, an excess amount of catalyst (e.g., 10 and 20 g) would reduce the concentration of the contaminant and O_3 reaction per unit area in considering the constant concentration of pollutants (Nie et al., 2012).

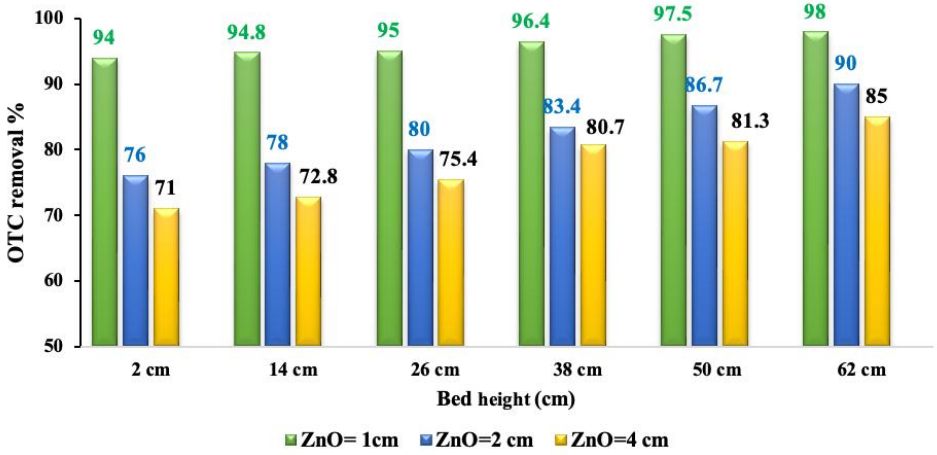

Figure 5. Effect of the catalyst bed height (ZnO) on the OTC removal efficiency.

3.4. Effect of Ozone Generation Rate

To determine the impact of ozone generation rate on the OTC degradation, the experiments were conducted at pH = 7, OTC load of 0.138, 0.69, and 1.38 mg/s, flow rates of 3.9 cm3/s, and bed heights of 1 cm. Results in Figure 6 show that increasing the initial ozone concentration improved the effectiveness of the degradation. Mechanistically, Ozone concentrations in the aqueous phase rise as a result of an increase in ozone gas concentration in the influent. This ozone either directly combines with OTC or breaks down to produce HO, which then reacts with the pollutant (Liu et al., 2009). Moreover, Figure 6 shows that the removal efficiency for OTC increases from 70% to 76% at 2 cm height, while the degradation efficiency increases from 83.4% to 90% at 62 cm height. This is due to the higher formation rate of ozone (e.g., rose from 0.138 mg/s to 1.38 mg/s). Thus, the increase in height and ozone rate can synergistically enhance the removal efficiency.

Also, when comparing the removal efficiency of the same height and different ozone generation rates, it can be found that the efficiency drops by not more than 6%. This demonstrated that the clearance rate is substantial even at low ozone concentrations, which is a cost-effective characteristic for ozonation-based antibiotic treatment. Ozone's volumetric mass transfer coefficient and mass transfer rate both rise with increasing ozone concentration. Lastly, increasing the amount of ozone that has been absorbed and reacts with OTC molecules can improve OTC decay (Wang et al., 2019b). This is consistent with what was reported by Reungoat et al. (2010), in a study including full-scale ozonation of secondary-treated wastewater (5 mgO_3/L and 15 min).

Also, when comparing the removal efficiency of the same height and different ozone generation rates, it can be found that the efficiency drops by not more than 6%. This demonstrated that the clearance rate is substantial even at low ozone concentrations, which is a cost-effective characteristic for ozonation-based antibiotic treatment. Ozone's volumetric mass transfer coefficient and mass transfer rate both rise with increasing ozone concentration. Lastly, increasing the amount of ozone that has been absorbed and reacts with OTC molecules can improve OTC decay (Wang et al., 2019b). This is consistent with what was reported by Reungoat et al. (2010), in a study including full-scale ozonation of secondary-treated wastewater (5 mgO_3/L and 15 min).

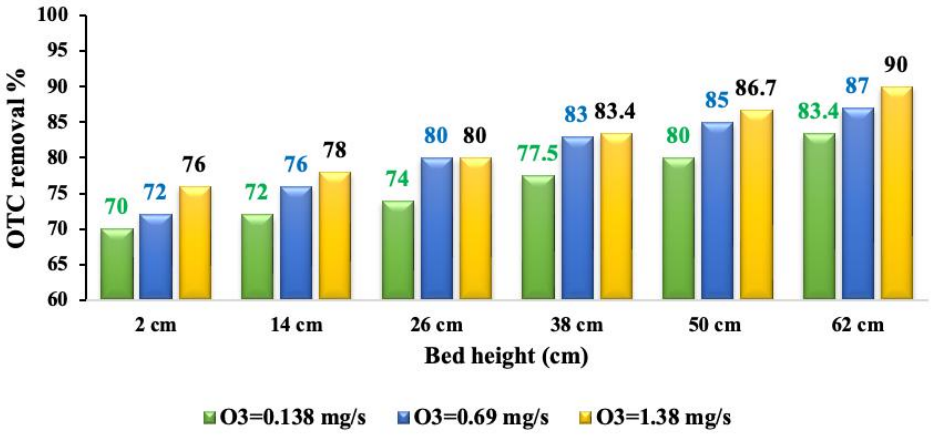

Figure 6. Effect of ozone generation rate on the OTC removal efficiency.

3.5. Evaluation of Ozone Self-decomposition Rate Constant (k_d s^{-1})

It will be agreed that non-reacting processes can transfer ozone mass through water microbubbles (Khuntia et al., 2013). In this study, the ozone self-decomposition rate constant (k_d) was established for this investigation by kinetic testing on the semi-batch reactor. The dissolved ozone absorption in water was measured and sustained until equilibrium was attained using the steady state of ozone concentration $[C_{AL}]$ss as a reference. Following that, ozone synthesis was stopped, and as can be seen in Figure 7, the amount of ozone in the reactor was reduced over the course of the experiment. It took less time for the ozone concentration to stabilize as the pH of the medium rose. The decomposition of ozone in water depends on the pH of the aqueous solution, and the kinetics of the first order have been followed (Khuntia et al., 2013).

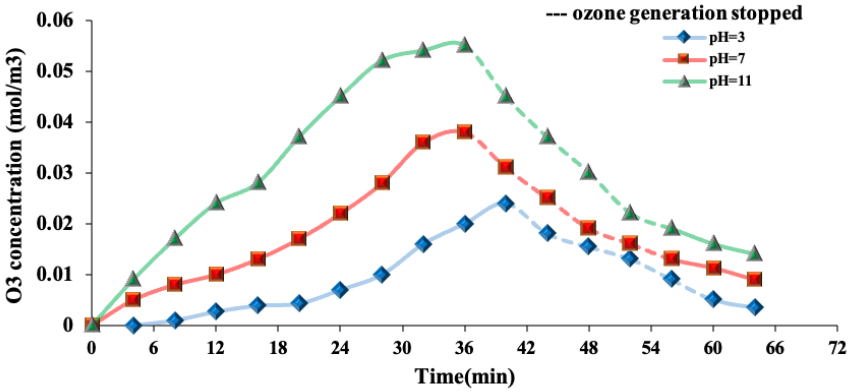

Figure 7. Concentration profiles of ozone during its self-decomposition.

The ozone equation auto-decomposition reaction rate can be written as follows (Kukuzaki et al., 2010):

$$\frac{d[C_{AL}]}{dt} = k_d[C_{AL} \quad (3)$$

Where $[C_{AL}]$ is the amount of ozone in the aqueous solution and k_d is the self-decomposition rate constant for ozone. Equation (3) is integrated with the boundary condition that $[C_{AL}]$= $[C_{AL}]$ss at time t = 0, and this results in the equation shown in Equation4 below:

$$ln\frac{[C_{AL}]ss}{[C_{AL}]} = k_d t \quad (4)$$

Equation (4) solved by (Microsoft Excel, 2013), predicts that k_d would be theslope of a straight line passing through the origin, and this line is a plot of Ln $[C_{AL}]$ss /$[C_{AL}]$ versus time t. Table 1 summarizes the experimental values of k_d at various pH levels.

k_d is a basic kinetic parameter, and it should be independent of the reactor type, On the other hand, it depended on the pH of the solution. Therefore, the values investigated in the literature proved wide variations from one experiment to another, for example k_d=4.2 x10^{-4} s^{-1} and k_{La}=5.4 x10^{-4} s^{-1} (pH unspecified) (Kukuzaki et al., 2010), k_d =(2.5 x10^4 -13.3 x10^4) s^{-1} at pH(6-9) (Khuntia et al., 2013), k_d=1.05 x10^{-3} s^{-1} and k_{La}=0.005 s^{-1}(pH=2.4) (Hai et al., 2012).

3.6. Absorption of Ozone

Ozone undergoes a slow decomposition reaction when it is absorbed into the water, implicated as a first-order kinetic. The following is a possible form for the mass balance for ozone absorption on the liquid phase (Grima, 2009):

$$k_{La}V_L(C_{AL}{}^{*}- C_{AL}) = V_L \frac{dC_{AL}}{dt} + V_L\, k_d\, C_{AL} \quad (5)$$

$$k_{La}C_{AL}{}^{*}- (k_{La} + k_d)\, C_{AL} = \frac{dC_{AL}}{dt} \quad (6)$$

$$\frac{dC_{AL}}{dt} = -(k_{La} + k_d)\, C_{AL} - \left(\frac{k_{La}}{k_{La}+k_d}\right) \quad (7)$$

Assume that:

$$K = k_{La} + k_d \text{ and } \alpha = \frac{k_{La}}{k_{La}+k_d} C_{AL}{}^{*} \quad (8)$$

Where K was the overall mass transfer coefficient s^{-1}

Equation 7 can then be rewritten as:

$$\frac{dC_{AL}}{dt} = -K(C_{AL} - \alpha) \quad (9)$$

$$\int_{C_{AL0}}^{C_{AL}} \frac{dC_{AL}}{C_{AL}-\alpha} = \int_0^t -K\, dt \quad (10)$$

$$ln\frac{C_{AL}-\alpha}{C_{AL0}-\alpha} = Kt \quad (11)$$

If $C_{AL0} = 0$

$$\frac{C_{AL}-\alpha}{-\alpha} = e^{-Kt} \quad (12)$$

$$C_{AL} = \alpha\,(-e^{-Kt}) \quad (13)$$

Or can be rewritten as:

$$C_{AL} = \frac{k_{La}}{K} C_{AL}{}^{*}\,(1- e^{-Kt}) \quad (14)$$

Where: k_d is the rate constant of ozone self-decomposition;

$K = k_{La} + k_d$,

k_{La} is the volumetric mass transfer coefficient (s^{-1}), C_{AL0} is the ozone concentration in the aqueous solution at $t = 0$ k_d was computed from a different exploratory investigation, $C_{AL}{}^{*}$, the saturation concentration of ozone was calculated from Figure 9 after 36 min at any pH value; the equilibrium concentration of ozone is reached.

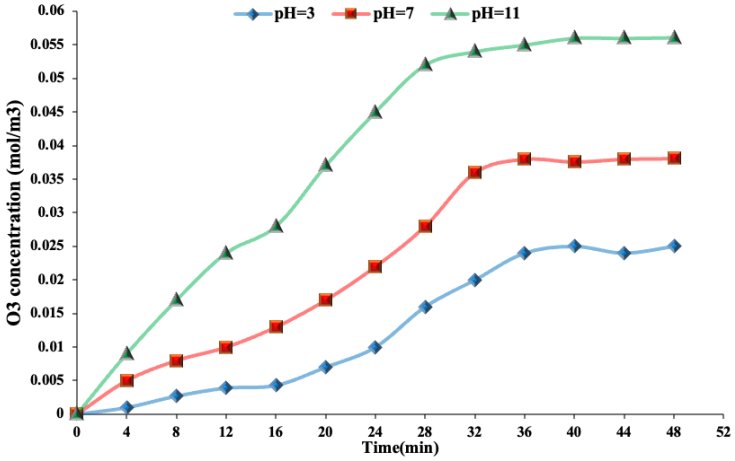

Figure 8. Dissolved ozone concentration in water at different pH and ozone generation rate=1.38 mg/s.

One of the factors that has a big impact on ozone damage is pH. In order to find out more about how pH affects the decomposition of ozone, several tests were conducted at various pH levels of 3, 7, and 11. When experiments were carried out without the introduction of any antibiotics, Figure 9 showed the effect of pH on the rates of ozone degradation. It was discovered that the degradation rate was minimal at low pH levels and increased as pH values increased. It takes some time for ozone absorption to steadily grow until it reaches saturation. The amount of ozone in water at saturation is represented by the symbol $C_{AL}{}^{*}$.

At any pH value, the equilibrium ozone concentration was attained in Figure 9 after 36 min. At pH (11), (7), and (3) correspondingly, the saturation concentrations of ozone were 0.055, 0.038, and 0.024 mol/m^3. The kinetic computation will be used to analyze the volumetric mass transfer coefficient for absorption processes at various pH levels. A straight line with a slope of k_{La} would have an origin and be a plot of $ln\frac{C_{AL}-C_{ALss}}{C_{AL0}-C_{ALss}}$ vs time (t).

Table 1 The experimental values of k_d, k_{La} *and* K at various pH

pH	3	7	11
$k_d\ s^{-1}$	0.08	0.111	0.216
$k_{La}\ s^{-1}$	0.04	0.055	0.108
$K\ s^{-1}$	0.12	0.166	0.324

Figure 10 to Figure 12 show the experimental and theoretical data that obtained from Equation 14 solved by Microsoft (Excel, 2013) at various pH (Grima, 2009):

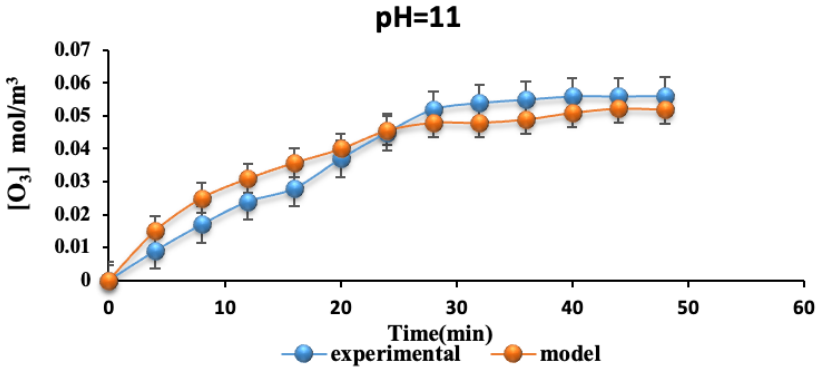

Figure 10. The experimental and theoretical data (pH=11, Ozonation rate= 1.38mg/s).

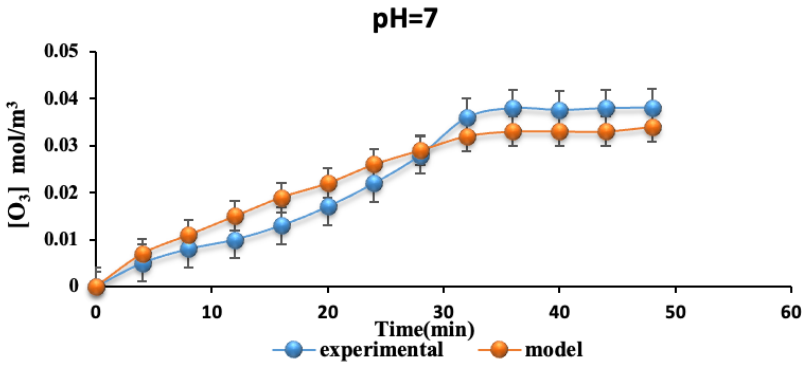

Figure 11. The experimental and theoretical data (pH=7, Ozonation rate =1.38mg/s).

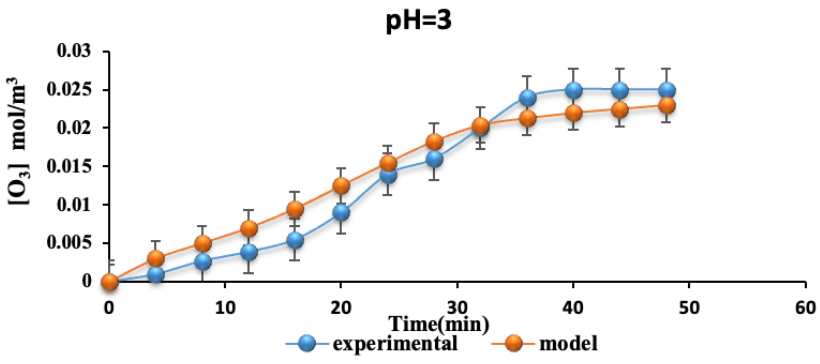

Figure 12. The experimental and theoretical data (pH=3, Ozonation rate =1.38mg/s).

The findings above clarified the impact of pH value on the constant rate of ozone absorption and breakdown at various pH levels. The constant rate of absorption increases when pH climbs to 11. In the ozone reaction pathway, pH was considered to be a crucial variable. In contrast to free-radical oxidation, which is more prevalent at higher pH levels, molecular ozone oxidation tends to predominate in acidic environments. This is due to the production of hydroxyl radicals ($OH^{\cdot}$), which is enhanced in an alkaline environment. Therefore, these radicals have a higher potential for oxidation than ozone molecules (Hoigné and Bader, 1983). The pH of the water has an impact on the solubility and rate of ozone breakdown. Because hydroxide ions have an impact on how ozone decomposes, the pH of the water is significant. As the solutions' alkalinity rises, so does their ozone content.

3.7. Kinetic Study

The kinetic study of the degradation process is a crucial step in determining the efficacy of the catalyst used and verifying its selectivity in the treatment system as a purified chemical. The kinetics of OTC degradation for SOP and COP were therefore explored in the current work, and the theoretical and experimental results are shown in Figures 13 and 14. According to coefficient determination values (R^2), the first and second order models' applicability and validation (Equations. 1 and 2) were assessed. However, the slope of the best fit line of the plot of Ln (C/Co) versus reaction time (t) was used to calculate the kinetic reaction rate parameter (k_a) for the first order model, while the slope of the best fit line of the plot of (1/C) was used to determine the parameter for the second order model. Table 2 and Table 3 contain a list of the outcomes for these parameters. As can be observed from the R^2 values of >0.9, the first order model adequately described the kinetic data in Figure 13. Additionally, the $k_a$values considerably rose during the catalytic ozonation process (Nasseh et al., 2020).

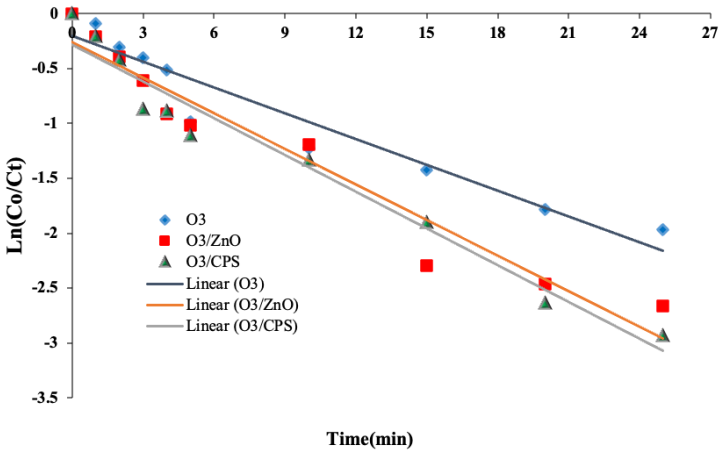

Figure 13. Testing first-order kinetics for OTC.

Table 2 The results of experimental kinetic data of degradation in SOP and COP reactions with the first-order equation

Type of process	Equation,where Y = Ln(C/Co), and x = t	k_a (1/min)	$t_{1/2}$(min)	R^2
O_3 only	Y = -0.0784 x - 0.2034	0.078	8.84	0.9269
O_3 /ZnO NPs	Y = -0.1083 x - 0.2541	0.108	6.39	0.9436
O_3 / CPS	Y = -0.1116 x - 0.2847	0.111	6.21	0.9629

In Figure 14, it can be seen that the R^2 values were obtained < 0.9 in testing the second order model for OTC degradation, and in Table 3 can be noted that the value of $t_{1/2}$ increased with decreasing k_a.

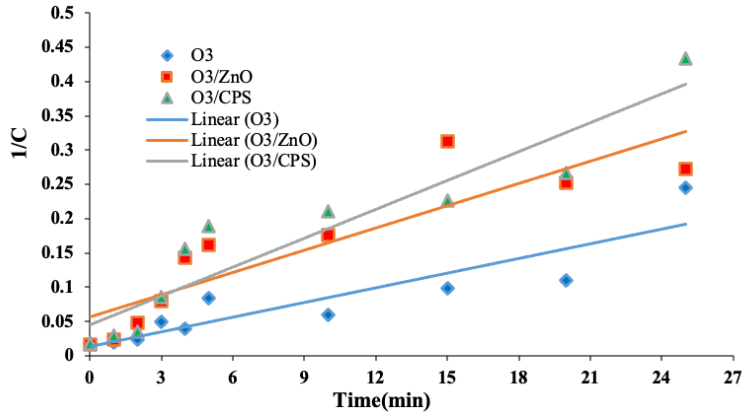

Figure 14. Testing second-order kinetics for OTC.

Table 3 The results of experimental kinetic data of degradation in SOP and COP reactions with the second-order equation

Type of process	Equation, where Y = Ln(C/Co), and x = t	k_a (1/min)	$t_{1/2}$(min)	R^2
O_3 only	y = 0.0071x + 0.0141	0.0071	97.6	0.8219
O_3 /ZnO NPs	y = 0.0109x + 0.056	0.0108	64.1	0.7912
O_3 / CPS	Y = 0.014 x + 0.0457	0.0140	49.34	0.8824

3.8. Changes in Toxicity

Staphylococcus aureus is a Gram-positive, round-shaped bacterium that is frequently found in the upper respiratory tract and on the skin and is a common cause of skin infections. The changes in the toxicity of the solution OTC and by-product were evaluated in different time intervals of ozonation processes for a concentration 50mg/L during 60 min on this bacterium were examined. must gather comprehensive data in order to emphasize if, during treatment, OTC is transformed into more harmful species or the original compound's toxic effects are lessened. The outcomes of the trials are depicted in Figure 15. After various treatment periods (5, 10, 20, 30, 40, 50, and 60) minutes, the bacterial growth appears to different extents. However, there is no bacterial growth in the zero zone (stock solution) of the sample. These findings demonstrate that the harmful parent molecule is present while the by-products are not.

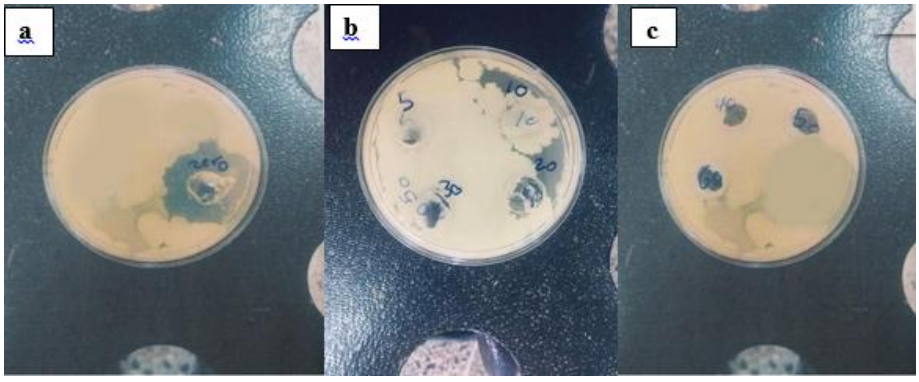

Figure 15. Change in toxicity of OTC solution: a) Before treatment with ozone at time 0, b) After treatment with ozone at time 5, 10, 20 and 30 min, c) After treatment with ozone at time 40, 50 and 60 min.

3.9. Gas Chromatography-Mass Spectrometry (GC-Mass) Analysis

Gas Chromatography-mass spectrometry is a technique that can be used to separate chemicals in a mixture or a sample and uses inert gases (like helium). It identifies any unknown chemical in the sample. Figure 16 shows the GC-Mass spectrum of OTC before treatment. The high peaks were observed at (19.986, 22.277, 17.323, and 20.373) at the area of 34.68, 29.59, 13.23 and 5.87%, respectively. The compounds of these peaks are fatty and carboxylic acids, including tridecanoic acid, methyl ester; 7-hexadecenoic acid, methyl ester, (z); cyclopentanetridecanoic acid, methyl ester, and pentadecanoic acid, methyl ester. Figure 17 shows the GC-Mass spectrum of OTC after treatment with ozone. Some peaks were increased in area as 19.986 and 17.323

that produced more fatty and carboxylic acids that causes the decreasing of pH value during ozonation process as (tridecanoic acid, methyl ester; 9-hexadecenoic acid, methyl ester (z); pentadecanoic acid, methyl ester). Some of peaks are decreased in area such as 23.171 and 26.614 that produced Oleyl alcohol, and Oleic acid that interned in olive oil that found in milk fat. These results were considered important for determining what is released into the aquatic environment. Figure 18 shows the mechanical GC-Mass analysis for the antibiotic oxy-tetracycline.

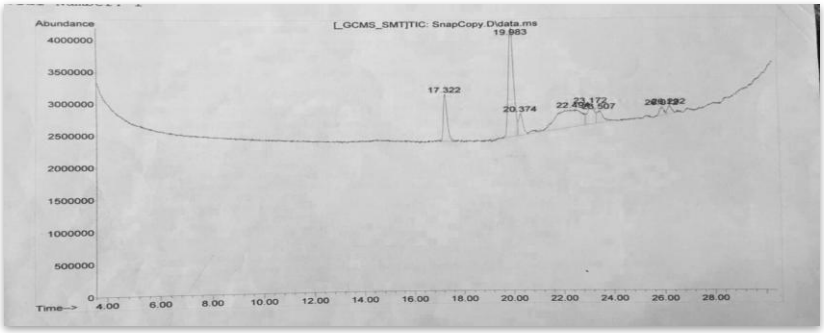

Figure 16. GC-Mass spectrum of OTC before treatment.

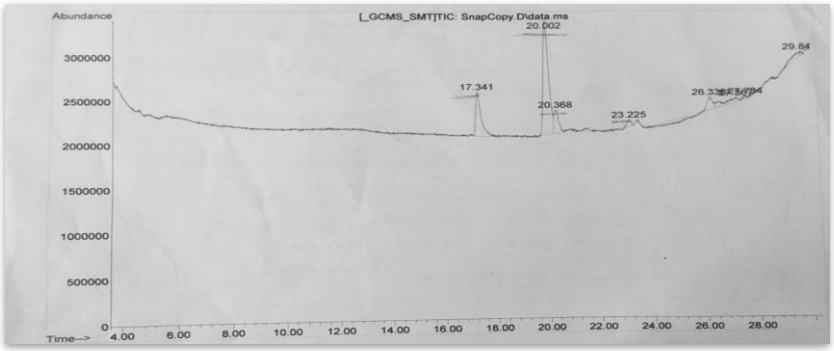

Figure 17. GC-Mass spectrum of OTC after treatment with ozone.

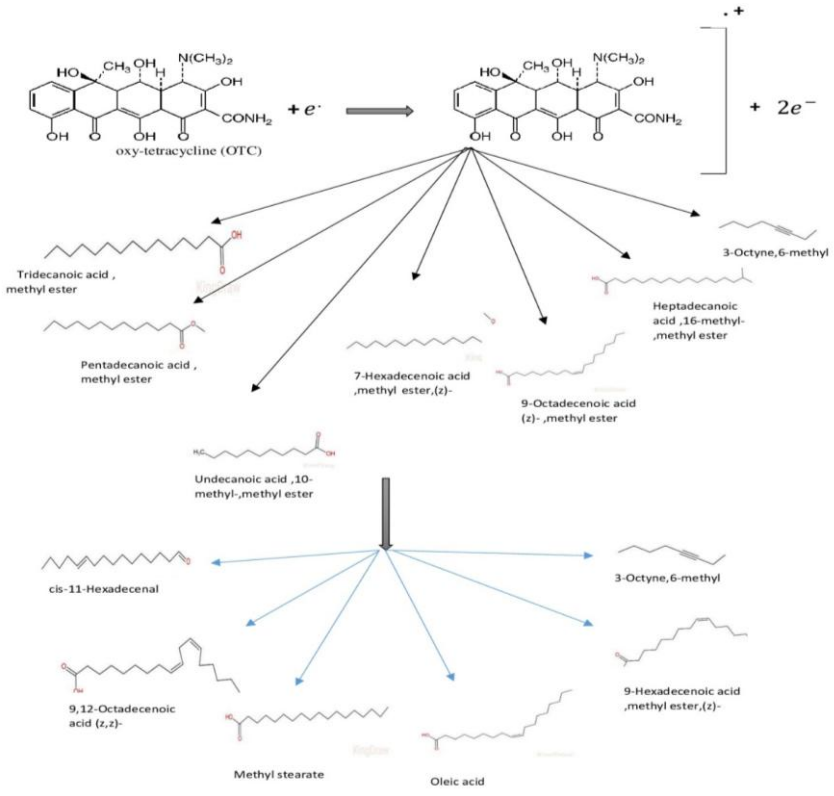

4. CONCLUSION

Catalytic ozonation of wastewater contaminated with Oxytetracycline (OTC) was conducted to evaluate the influence of ZnO NPs on the removal efficiency of OTC. The results indicated that continuous catalytic ozonation by ZnO could be an efficient treatment for degrading oxy-tetracycline in comparison with the sole ozonation process. Best conditions for OTC degradation process by catalytic ozonation to obtain maximum efficiency of (98%) in a continuous reactor using ozone generation rate=1.38 mg/sec, flow rate=3.9 cm^3/sec and bed height =1cm. GC-Mass analysis showed that fatty, carboxylic acids, oleyl alcohol, and oleic acid were produced as byproducts from the degradation of OTC. At low pH, the decay rate was slow due to fewer radicals (OH) and thus lower OTC degradation, and it increased as the pH increased. The reaction follows first-order kinetics with $R^2 > 0.9$. The outcomes of this study provide insight into catalytic ozonation augmented with ZnO NPs in OTC removal applications.

REFERENCES

[1] Al-Anssari, S., Shanshool, H. A., Keshavarz, A. & Sarmadivaleh, M. 2020. Synergistic effect of hydrophilic nanoparticles and anionic surfactant on the stability and viscoelastic properties of oil in water (o/w) emulations; application for enhanced oil recovery (EOR). Journal of Petroleum Research and Studies, 10**,** 33-53.

[2] Al-Anssari, S. F. J. 2018. *Application of Nanotechnology in Chemical Enhanced Oil Recovery and Carbon Storage.* Curtin University.

[3] Al-Bayati, I. S., Mohammed, S. A. M. & Al-Anssari, S. Recovery of methyl orange from aqueous solutions by bulk liquid membrane process facilitated with anionic carrier. AIP Conference Proceedings, 2023. AIP Publishing.

[4] Al Jibouri, A. K. H., Wu, J. & Upreti, S. R. 2015. Continuous ozonation of methylene blue in water. *Journal of Water Process Engineering,* 8**,** 142-150.

[5] Alwared, A. I., Mohammed, N. A., Al-Musawi, T. J. & Mohammed, A. A. 2023. Solar-induced photocatalytic degradation of reactive red and turquoise dyes using a titanium oxide/xanthan gum composite. *Sustainability,* 15**,** 10815.

[6] Balaji, T., Yulia, B., Atikur, R., Saiful, I., Mizanur, R., Azharul, I., Joslyn, P., James, K., Jasmine, T., Dhananjay, K., Shamsuddin, I. & Debasish, K. 2011. Development of Mesoporous Silica Encapsulated Pd-Ni Nanocatalyst for Hydrogen Production. *Production and Purification of Ultraclean Transportation Fuels.* American Chemical Society.

[7] Baruah, S. & Dutta, J. 2009. Hydrothermal growth of ZnO nanostructures. *Science and Technology of Advanced Materials,* 10**,** 013001.

[8] Buxton, G. V., Greenstock, C. L., Phillips Helman, W. & Ross, A. B. 1988. Critical review of rate constants for reacitons of hydrated electrons. *J. Phys. Chem. Ref. Data;(United States),* 17.

[9] Grima, N. 2009. *Kinetic and mass transfer studies of ozone degradation of organics in liquid/gas-ozone and liquid/solid-ozone systems.* University of Bradford.

[10] Hai, J., Zhang, G. & Cheng, J. 2012. Estimation of mass transfer coefficient in ozone absorption by linear least square fitting and Simplex search methods. *Journal of Central South University,* 19**,** 3396-3399.

[11] Hammood, Z. A. & Mohammed, A. A. 2024a. Enhanced adsorption of ciprofloxacin from an aqueous solution using a novel CaMgAl-layered double hydroxide/red mud composite. *Results in Engineering,* 23**,** 102600.

[12] Hammood, Z. A. & Mohammed, A. A. 2024b. Understanding the sorbent properties of layered double hydroxide for the removal of pharmaceuticals from aqueous Solutions: A comprehensive review. *Results in Chemistry***,** 101952.

[13] Hernandez, R., Zappi, M., Colucci, J. & Jones, R. 2002. Comparing the performance of various advanced oxidation processes for treatment of acetone contaminated water. *Journal of hazardous materials,* 92**,** 33-50.

[14] Hoigné, J. & Bader, H. 1983. Rate constants of reactions of ozone with organic and inorganic compounds in water—I: non-dissociating organic compounds. *Water Research,* 17**,** 173-183.

[15] Homem, V. & Santos, L. 2011. Degradation and removal methods of antibiotics from aqueous matrices–a review. *Journal of environmental management,* 92**,** 2304-2347.

[16] Kerdnawee, K., Kuptajit, P., Sano, N., Tamon, H., Chaiwat, W. & Charinpanitkul, T. 2017. Catalytic ozonation of oxy-tetracycline using magnetic carbon nanoparticles. *Journal of the Japan Institute of Energy,* 96**,** 362-366.

[17] Khuntia, S., Majumder, S. K. & Ghosh, P. 2013. Removal of ammonia from water by ozone microbubbles. *Industrial & Engineering Chemistry Research,* 52**,** 318-326.

[18] Kim, S., Eichhorn, P., Jensen, J. N., Weber, A. S. & Aga, D. S. 2005. Removal of antibiotics in wastewater: effect of hydraulic and solid retention times on the fate of tetracycline in the activated sludge process. *Environmental science & technology,* 39**,** 5816-5823.

[19] Kimera, Z. I., Mdegela, R. H., Mhaiki, C. J., Karimuribo, E. D., Mabiki, F., Nonga, H. E. & Mwesongo, J. 2015. Determination of oxytetracycline residues in cattle meat marketed in the Kilosa district, Tanzania: research communication. *Onderstepoort Journal of Veterinary Research,* 82**,** 1-5.

[20] Kukuzaki, M., Fujimoto, K., Kai, S., Ohe, K., Oshima, T. & Baba, Y. 2010. Ozone mass transfer in an ozone–water contacting process with Shirasu porous glass (SPG) membranes—A comparative study of hydrophilic and hydrophobic membranes. *Separation and purification technology,* 72**,** 347-356.

[21] Li, K., Yediler, A., Yang, M., Schulte-Hostede, S. & Wong, M. H. 2008. Ozonation of oxytetracycline and toxicological assessment of its oxidation by-products. *Chemosphere,* 72**,** 473-478.

[22] Liu, Z.-H., Kanjo, Y. & Mizutani, S. 2009. Removal mechanisms for endocrine disrupting compounds (EDCs) in wastewater treatment—physical means, biodegradation, and chemical advanced oxidation: a review. *Science of the total environment,* 407**,** 731-748.

[23] Mahdi, M., Al-Anssari, S. & Arain, Z.-U.-A. 2023. Influence of nanofluid flooding on oil displacement in porous media. *Iraqi Journal of Chemical and Petroleum Engineering,* 24**,** 19-30.

[24] Mohammed, A. A., Al-Musawi, T. J., Kareem, S. L., Zarrabi, M. & Al-Ma'abreh, A. M. 2020a. Simultaneous adsorption of tetracycline, amoxicillin, and ciprofloxacin by pistachio shell powder coated with zinc oxide nanoparticles. *Arabian Journal of Chemistry,* 13**,** 4629-4643.

[25] Mohammed, A. A., Atiya, M. A. & Hussein, M. A. 2020b. Simultaneous studies of emulsion stability and extraction capacity for the removal of tetracycline from aqueous solution by liquid surfactant membrane. *Chemical Engineering Research and Design,* 159**,** 225-235.

[26] Mohammed, A. A., Atiya, M. A. & Hussein, M. A. 2020c. Studies on membrane stability and extraction of ciprofloxacin from aqueous solution using pickering emulsion liquid membrane stabilized by magnetic nano-Fe2O3. *Colloids and Surfaces A: Physicochemical and Engineering Aspects,* 585**,** 124044.

[27] Mohan, A. C. & Renjanadevi, B. 2016. Preparation of Zinc Oxide Nanoparticles and its Characterization Using Scanning Electron Microscopy (SEM) and X-Ray Diffraction(XRD). *Procedia Technology,* 24**,** 761-766.

[28] Mohsin, M. K. & Mohammed, A. A. 2021. Catalytic ozonation for removal of antibiotic oxy-tetracycline using zinc oxide nanoparticles. *Applied Water Science,* 11**,** 9.

[29] Nashmi, O. A., Mohammed, A. A. & Abdulrazzaq, N. N. 2020. Investigation of ozone microbubbles for the degradation of methylene orange contaminated wastewater. *Iraqi Journal of Chemical and Petroleum Engineering,* 21**,** 25-35.

[30] Nasseh, N., Arghavan, F. S., Rodriguez-Couto, S., Panahi, A. H., Esmati, M. & A-Musawi, T. J. 2020. Preparation of activated carbon@ ZnO composite and its application as a novel catalyst in catalytic ozonation process for metronidazole degradation. *Advanced Powder Technology,* 31**,** 875-885.

[31] Nie, Y., Xing, S., Hu, C. & Qu, J. 2012. Efficient Removal of Toxic Pollutants Over Fe–Co/ZrO 2 Bimetallic Catalyst with Ozone. *Catalysis letters,* 142**,** 1026-1032.

[32] Padmavathy, N. & Vijayaraghavan, R. 2008. Enhanced bioactivity of ZnO nanoparticles—an antimicrobial study. *Science and Technology of Advanced Materials,* 9**,** 035004.

[33] Reungoat, J., Macova, M., Escher, B. I., Carswell, S., Mueller, J. F. & Keller, J. 2010. Removal of micropollutants and reduction of biological activity in a full scale reclamation plant using ozonation and activated carbon filtration. *Water research,* 44**,** 625-637.

[34] Roy, N. & Chakraborty, S. 2021. ZnO as photocatalyst: An approach to waste water treatment. *Materials Today: Proceedings,* 46**,** 6399-6403.

[35] Sarmah, A. K., Meyer, M. T. & Boxall, A. B. 2006. A global perspective on the use, sales, exposure pathways, occurrence, fate and effects of veterinary antibiotics (VAs) in the environment. *Chemosphere,* 65**,** 725-759.

[36] Sun, Q., Lu, J., Wu, J. & Zhu, G. 2019. Catalytic ozonation of sulfonamide, fluoroquinolone, and tetracycline antibiotics using nano-magnesium hydroxide from natural bischofite. *Water, Air, & Soil Pollution,* 230**,** 1-15.

[37] Wang, D., Li, J., Xu, Z., Zhu, Y. & Chen, G. 2019a. Preparation of novel flower-like BiVO4/Bi2Ti2O7/Fe3O4 for simultaneous removal of tetracycline and Cu2+: adsorption and photocatalytic mechanisms. *Journal of Colloid and Interface Science,* 533**,** 344-357.

[38] Wang, H., Zhang, M., He, X., Du, T., Wang, Y., Li, Y. & Hao, T. 2019b. Facile prepared ball-like TiO2 at GO composites for oxytetracycline removal under solar and visible lights. *Water research,* 160**,** 197-205.

[39] Wang, J. L. & Xu, L. J. 2012. Advanced oxidation processes for wastewater treatment: formation of hydroxyl radical and application. *Critical reviews in environmental science and technology,* 42**,** 251-325.

[40] Zhu, J., Snow, D. D., Cassada, D., Monson, S. & Spalding, R. 2001. Analysis of oxytetracycline, tetracycline, and chlortetracycline in water using solid-phase extraction and liquid chromatography–tandem mass spectrometry. *Journal of Chromatography A,* 928**,** 177-186.